CHIN. PHYS. LETT. Vol. 38, No. 12 (2021) 121401 **Express Letter**

Pauli Radius of the Proton

Zhu-Fang Cui(崔著钫)[1,2], Daniele Binosi[3*], Craig D. Roberts[1,2*], and Sebastian M. Schmidt[4,5]

[1]*School of Physics, Nanjing University, Nanjing 210093, China*
[2]*Institute for Nonperturbative Physics, Nanjing University, Nanjing 210093, China*
[3]*European Centre for Theoretical Studies in Nuclear Physics and Related Areas, Villa Tambosi, Strada delle Tabarelle 286, I-38123 Villazzano (TN), Italy*
[4]*Helmholtz-Zentrum Dresden-Rossendorf, Dresden D-01314, Germany*
[5]*RWTH Aachen University, III. Physikalisches Institut B, Aachen D-52074, Germany*

(Received 7 September 2021; accepted 8 November 2021; published online 13 November 2021)

Using a procedure based on interpolation via continued fractions supplemented by statistical sampling, we analyze proton magnetic form factor data obtained via electron+proton scattering on $Q^2 \in [0.027, 0.55]\,\mathrm{GeV}^2$ with the goal of determining the proton magnetic radius. The approach avoids assumptions about the function form used for data interpolation and ensuing extrapolation onto $Q^2 \simeq 0$ for extraction of the form factor slope. In this way, we find $r_{\mathrm{M}} = 0.817(27)\,\mathrm{fm}$. Regarding the difference between proton electric and magnetic radii calculated in this way, extant data are seen to be compatible with the possibility that the slopes of the proton Dirac and Pauli form factors, $F_{1,2}(Q^2)$, are not truly independent observables; to wit, the difference $F_1'(0) - F_2'(0)/\kappa_{\mathrm{p}} = [1+\kappa_{\mathrm{p}}]/[4m_{\mathrm{p}}^2]$, viz., the proton Foldy term.

DOI: 10.1088/0256-307X/38/12/121401

1. Introduction. The Universe is 14-billion years old. In all that time, proton decay has not been observed. This remarkable fact makes the proton Nature's most fundamental bound state. It is also a fermion; hence, owing to the spin-statistics theorem,[1] the proton is an essentially quantum field theoretical composite object because:[2] "...the connection between spin and statistics is one of the most important applications of the special relativity theory..."; and quantum field theory is the only known means of unifying quantum mechanics with special relativity.[3] The remaining Poincaré-invariant observable associated with an asymptotic proton state is its mass,[4] m_{p}, which is known with a relative uncertainty of $\sim 10^{-10}$.[5]

The proton has electric charge $e_{\mathrm{p}} = +1$, so electron+proton (ep) scattering has long been used to probe its dynamical properties; and being a relativistic composite object, the proton's electromagnetic current involves two form factors, Dirac F_1 and Pauli F_2:[6–11]

$$J_\mu(Q) = i e_{\mathrm{p}} \bar{u}(P') \Lambda_\mu(Q) u(P), \tag{1a}$$

$$\Lambda_\mu(Q) = \gamma_\mu F_1(Q^2) + \frac{1}{2m_{\mathrm{p}}} \sigma_{\mu\nu} Q_\nu F_2(Q^2), \tag{1b}$$

where $Q = P' - P$, with P and P' being the incoming/outgoing proton momenta in the scattering process. The proton electric and magnetic form factors are

$$G_{\mathrm{E}} = F_1 - \frac{Q^2}{4m_{\mathrm{p}}^2} F_2, \quad G_{\mathrm{M}} = F_1 + F_2. \tag{2}$$

Three-dimensional Fourier transforms of $G_{\mathrm{E,M}}$ were long interpreted as clean measures of the spatial distributions of electric charge and magnetization inside the proton,[12] with the associated radii given by

$$r_{\mathrm{E,M}}^2 = \left[\frac{-6}{G_{\mathrm{E,M}}(Q^2)} \frac{d}{dQ^2} G_{\mathrm{E,M}}(Q^2) \right]_{Q^2=0}. \tag{3}$$

Today, although their interpretation has changed,[13] the importance of measuring these key dynamical characteristics of the proton has not.

For a structureless, noninteracting fermion, the Dirac equation yields $F_2 \equiv 0 \Rightarrow G_{\mathrm{E}} \equiv G_{\mathrm{M}}$; and perturbative corrections in quantum electrodynamics (QED) only introduce small modifications for elementary fermions.[14,15] Any material differences between G_{E} and G_{M} are marks of compositeness, and the first signal of this for the proton was found in the discovery that its anomalous magnetic moment $\kappa_{\mathrm{p}} := \mu_{\mathrm{p}} - 1 := F_2(0) \approx 2$.[16] Notwithstanding that, until the beginning of the current millennium, available ep scattering data were consistent with $\mu_{\mathrm{p}} G_{\mathrm{E}}(Q^2)/G_{\mathrm{M}}(Q^2) = 1$; and it was only the operation of an electron accelerator with the combination of high energy, luminosity, and beam polarisation that revealed $\mu_{\mathrm{p}} G_{\mathrm{E}}(Q^2)/G_{\mathrm{M}}(Q^2) \neq 1$.[17] This being the case, then the proton electric and

Supported by the National Natural Science Foundation of China (Grant Nos. 12135007 and 11805097), the Natural Science Foundation of Jiangsu Province, China (Grant No. BK20180323), and STRONG-2020, "the strong interaction at the frontier of knowledge: fundamental research and applications" which received funding from the European Union's Horizon 2020 Research and Innovation Programme (Grant No. 824093).
*Corresponding authors. Email: binosi@ectstar.eu; cdroberts@nju.edu.cn
© 2021 Chinese Physical Society and IOP Publishing Ltd

magnetic radii must be different; unless some dynamical mechanism leads to

$$\frac{F_2'(0)}{\kappa_{\rm p}} = F_1'(0) - \frac{\mu_{\rm p}}{4m_{\rm p}^2}. \tag{4}$$

Equation (4) states that the proton's Pauli and Dirac radii are not independent observables. Rather, their difference is always positive, being fixed by the proton Foldy term.[18] Should this be true, then the proton's light-front transverse mean-square magnetic radius,[13] $b_{\rm M}^{\perp}$, is a known quantity once its mean-square charge radius, $b_{\rm E}^{\perp}$, is determined, with no additional input necessary; and $b_{\rm M}^{\perp} > b_{\rm E}^{\perp}$. This last feature was discussed in Ref. [19]. Of course, one could instead describe $b_{\rm E}^{\perp}$ as the contingent quantity.

No symmetry considerations require Eq. (4); thus, the result can only emerge as a consequence of Standard Model dynamics. One might therefore ask for the status of Eq. (4) in theory; but the precision of today's theory is insufficient to deliver an answer.

Following a decade of controversy, experiment is settling on a value for the proton electric radius,[20–26] with a recent assessment listing the following value:[5]

$$r_{\rm E} = 0.8409(4)\,{\rm fm}. \tag{5}$$

However, as emphasized by Fig. 1, the value of the proton magnetic radius is far less certain. The most precise available data were collected by the A1 Collaboration;[27,28] but as highlighted by entries [B, C] in Fig. 1, applying the same analysis method to the world's data when including/excluding the A1 set can lead to mutually inconsistent results. The particle data group (PDG)[5] quotes an average of [B, C] in Fig. 1:

$$r_{\rm M} = 0.851 \pm 0.026\,{\rm fm}. \tag{6}$$

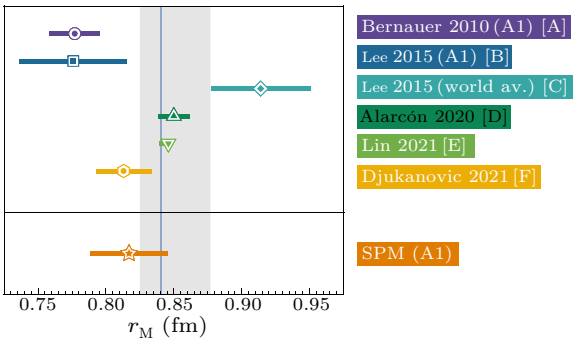

Fig. 1. Upper panel: Proton $r_{\rm M}$ extractions, obtained with various techniques: [A] = Refs. [27,28] (A1 Collaboration); [B] = Ref. [29] (A1 data); [C] = Ref. [29] (world average omitting A1 data); [D] = Ref. [30] (dispersion theory); [E] = Ref. [31] (dispersion theory); [F] = Ref. [32] (lattice quantum chromodynamics). The light-grey band is Eq. (6); within mutual uncertainties, this value agrees with $r_{\rm E}$ in Eq. (5), which is indicated by the thin vertical blue band. Lower panel: Result in Eq. (10), obtained from the data in Ref. [27] using the Schlessinger point method (SPM)[33–35] as described herein.

The proton radius controversy[36] demonstrated that a sound extraction of hadron radii from form factors measured in lepton+hadron scattering requires precise data, densely packed at very low Q^2. Furthermore, in the analysis of that data, great care should be taken to eliminate all systematic error intrinsic to the choice of data fitting function.[37–45]

Recently, a scheme was developed to circumvent any need for a specific choice of fitting function in analyzing form factor data.[46,47] Introduced in Refs. [33,34] and now often described as the statistical SPM, it has been honed in hadron physics applications, especially those which require interpolation and reliable extrapolation, e.g., Refs. [48-54]. The SPM builds form-unbiased interpolations of data as the foundation for well constrained extrapolations. Herein, we employ it to extract $r_{\rm M}$ from the A1 data.[27,28]

Before proceeding, it is worth remarking that the efficacy of the SPM rests firmly upon its mathematical connection with the Padé approximant. Indeed, the procedure might equally be called the multipoint Padé approximants technique. Owing to the properties of analytic functions, then with $N > 0$ perfect values of such a function, f, at discrete real points, $\mathcal{D} = \{x_i \,|\, i = 1, \ldots, N\}$, the SPM will return an accurate representation of $f(x)$ within a radius of convergence fixed by that one of the function's branch points which lies closest to the domain $\mathcal{D}$. A simple example is provided by a monopole: $f(x) = 1/(1+x)$, represented by N points, each one lying on the curve, with N large. Using any one of those points, the SPM will exactly reproduce $f(x)$.

To counter the problem that perfect function values are impossible to obtain, a powerful statistical aspect may be introduced. Namely, one chooses $M \lesssim N/2$ points at random from $\mathcal{D}$ and considers the associated function values. Using the SPM with each pair, $[x_i, f(x_i)]$, one obtains a collection of analytic approximations to the monopole whose spread measures the uncertainty inherent in the numerical calculation. Each one of the approximations is of practically equal quality to the best least-squares fit to f as defined by the points in $\mathcal{D}$. There is no qualitative difference when extending these ideas to more sophisticated functions.

Naturally, dealing with such "imperfections" is crucial when treating experimental data, as is the introduction of the smoothing procedure described below.

2. SPM and Proton Form Factor Data. The data obtained by the A1 Collaboration relate simultaneously to the proton electric and magnetic radii. They comprise 1400 cross-sections measured with beam energies (in GeV): 0.18, 0.315, 0.45, 0.585, 0.72, 0.855. Focusing on the electric form factor, Ref. [46] worked with $N = 40$ cross-section points in the low-Q^2 interval: $3.8 \times 10^{-3} \leq Q^2/{\rm GeV}^2 \leq 1.4 \times 10^{-2}$; and applied

to this data, the SPM yielded:

$$r_{\rm E}^{\rm A1\text{-}SPM} = 0.856 \pm 0.014_{\rm stat}\,{\rm fm}. \tag{7}$$

Since details are available in Ref. [46] hereafter we only sketch the SPM via its use in extracting $r_{\rm M}$.

Regarding A1 data on the magnetic form factor, one finds in the Supplementary Material of Ref. [28] 77 points describing a Rosenbluth separation[55] of the *ep* cross-sections into results for $G_{\rm E,M}$ on the domain $1.5\times10^{-2} \leq Q^2/{\rm GeV}^2 \leq 0.55$. The first nine $G_{\rm M}$ points are too noisy to be useful, only adding uncertainty to the SPM result without altering the central value; so herein we report an analysis of the $N = 68 G_{\rm M}$ data on the domain $\mathcal{D}_{A1} = \{Q^2\,|\,2.7\times10^{-2} \leq Q^2/{\rm GeV}^2 \leq 0.55\}$.

In implementing the SPM, one constructs a prodigious number of continued fraction interpolations, every one encapsulating both local and global aspects of the curve underlying the data. The global quality is vital because it justifies use of the interpolations outside the domain of available data and thus enables and legitimizes evaluation of the curves' slope at the origin, i.e., use of Eq. (3).

Of course, good data are statistically scattered around that curve which properly represents the form factor whose measurement is the aim; hence, they should not be directly interpolated. We address this issue by *smoothing* with a *roughness penalty*, following the procedure explained in Ref. [56] and made concrete in Section 3 of Ref. [46]. The approach is characterized by a well-defined optimal roughness penalty, ϵ, whose value is a self-consistent output of the smoothing procedure: $\epsilon = 0$ means that the data are untouched by smoothing whilst $\epsilon = 1$ returns a linear least-squares realignment of the data. In the case of $r_{\rm E}$, considered in Ref. [46] and $r_{\rm M}$, herein, $\epsilon \simeq 0$.

The $\mathcal{D}_{A1}$ set has $N = 68$ points. From the data on $\mathcal{D}_{A1}$, we randomly select L elements, with $7 \leq L \leq 19$. With a given value of L, one can generate $C(N,L)$ different interpolating functions, i.e., $O(9.7\times10^8 - 3.3\times10^{15})$ interpolators. From the collection obtained using a given value of L, we select the first 5000 that are smooth on the entire Q^2 domain covered by the data. Every interpolating function defines an extrapolation to $Q^2 = 0$, wherefrom $r_{\rm M}$ can be obtained via Eq. (3). So, for each value of L, $r_{\rm M}$ is determined by the average of all results computed from the 5000 curves.

To estimate the uncertainty in a particular SPM-determined value of $r_{\rm M}$, one must first reckon with the experimental error in the data. This is achieved herein by using a statistical bootstrap procedure.[57] We generate 1 000 copies of the set by replacing each element by a new point, distributed randomly about the mean defined by the element itself with variance equal to its associated error. Additionally, since L is changed, there is a second error source $\sigma_{\delta L}$, which can be estimated by shifting $L \to L'$, repeating all steps for this new L'-value, and computing the standard deviation of the distribution of $r_{\rm M}^L$ for different L values.

Accordingly, one arrives at the SPM result: $r_{\rm M} \pm \sigma_r$;

$$r_{\rm M} = \sum_{j=1}^{4} \frac{r_{\rm M}^{L_j}}{4}; \quad \sigma_r = \Big[\sum_{j=1}^{4} \frac{(\sigma_r^{L_j})^2}{4^2} + \sigma_{\delta L}^2\Big]^{1/2}. \tag{8}$$

For reasons explained below, we calculate results for each one of the values L in $\mathcal{S}_L = \{L_j = 3+4j\,|\,j = 1,2,3,4\}$. Thus, we have 20-million results for $r_{\rm M}$, each computed from an independent interpolation. For all j values in the range specified above, $\sigma_{\delta L} \ll \sigma_r^{L_j}$; hence, the result is largely independent of the chosen value of L.

3. Validation of SPM Extrapolation on A1 Data. The keystone of any SPM data analysis is validation on the set. Herein, this means demonstrating that the radius returned by the SPM is reliable when used in connection with data on $\mathcal{D}_{A1}$. We accomplish this using the approach explained in the Supplementary Material of Ref. [46].

Step 1. The A1 Collaboration employed ten distinct data fitting models as the means by which to infer a result for $r_{\rm M}$.[28] From this collection, we selected the seven that are most straightforward to implement: (i) dipole; (ii) double dipole; (iii) polynomial; (iv) polynomial plus dipole; (v) polynomial times dipole; (vi) inverse polynomial; and (vii) Friedrich–Walcher parametrization.[58] Each of these models is connected with a distinct magnetic radius,[28] which defines the target input radius, $r_{\rm M}^{\rm input}$, that is, the SPM should recover (in fm): $r_{\rm M}^{\rm i} = 0.85$; $r_{\rm M}^{\rm ii} = 0.838761$; $r_{\rm M}^{\rm iii} = 0.779342$; $r_{\rm M}^{\rm iv} = 0.778892$; $r_{\rm M}^{v} = 0.775504$; $r_{\rm M}^{\rm vi} = 0.768562$; $r_{\rm M}^{\rm vii} = 0.807416$. Using every one of these models, we generated replicas of the A1 data built from the model values of $G_{\rm M}$ evaluated at the Q^2 points in $\mathcal{D}_{A1}$. The character of real data was modeled by scattering the values in response to fluctuations drawn according to a normal distribution.

Step 2. Treating each of the seven sets as real, we determined the radius as described above. (Ⅰ) Generate 10^3 replicas. (Ⅱ) Smooth each replica with the optimal parameter. (Ⅲ) Use the SPM to obtain $r_{\rm M}^{L_j}$ and $\sigma_{\rm M}^{L_j}$, varying the number of input points $\{L_j = 3+4j\,|\,j = 1,2,3,4\}$. (Ⅳ) Compute the final SPM result via Eq. (8) and compare it with the input value.

The results of validation are summarized as follows:

[A] For a given value of $L \in \mathcal{S}_L$ and all seven forms of fitting model, the distribution of SPM-extracted radii is a Gaussian, which is centered on the radius input value and whose characteristics are practically independent of L: in these cases, $\sigma_{\delta L} \ll \sigma_r^{L_j}$. We also considered $L \in \mathcal{O}_L = \{M_{ji} = 3+4j+i\,|\,j = 1,2,3, i = 1,2,3\}$. In these instances, however, one does not recover a satisfactory Gaussian distribution.

So, we omit them from further consideration; to wit, we allow the validation process to impose a subset of L-values on our analysis, viz., $L \in \mathcal{S}_L$.

[B] Defining the bias: $\delta r_{\rm M} = r_{\rm M} - r_{\rm M}^{\rm input}$, then the SPM extraction of the proton magnetic radius is robust: typically, $|\delta r_{\rm M}| \lesssim \sigma_r$, where σ_r is the standard error in Eq. (8). The inverse polynomial model is the worst case. These remarks are illustrated in Fig. 2, which depicts $\delta r_{\rm M}$ as obtained using the SPM to recover $r_{\rm M}$ from each one of the seven $G_{\rm M}$ generators with their distinct $r_{\rm M}^{\rm input}$ values.

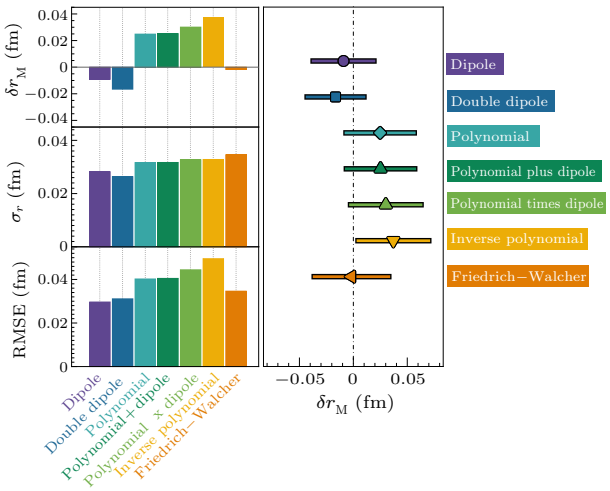

Fig. 2. Top and right panels: bias, $\delta r_{\rm M} = r_{\rm M} - r_{\rm M}^{\rm input}$, where the values of $r_{\rm M}^{\rm input}$ are listed in step 1. Middle panel: standard error, Eq. (8). Bottom panel: RMSE, Eq. (9), for SPM extractions of the proton magnetic radius from 5000 replicas built using the seven models employed by the A1 Collaboration.[28]

[C] Considering the root-mean-square error:

$$\text{RMSE} = \sqrt{(\delta r_{\rm M})^2 + \sigma_r^2}\,, \tag{9}$$

then, as revealed in Fig. 2, the SPM produces RMSE values which are approximatively independent of the model used to build the replicas. It therefore satisfies a standard "goodness-of-fit" criterion.[59] Hence, the SPM extraction of $r_{\rm M}$ may objectively be judged to return a reliable expression of the information contained in the data.

4. Proton Magnetic Radius from A1 Data. With the SPM now shown to return a reliable radius result from A1-like data, with its quoted errors, we turn to the real data on $\mathcal{D}_{A1}$ and obtain:

$$r_{\rm M}^{\text{A1-SPM}} = 0.817 \pm 0.027_{\rm stat}. \tag{10}$$

As evident in Fig. 1, within mutual uncertainties, this result agrees with that reported in Ref. [27], but the central value is 5.1% larger. This contrasts with our kindred extraction of $r_{\rm E}$ from A1 data, discussed elsewhere.[46] In that case, the central result from Eq. (7) is 2.6% lower.

These differences have meaning in connection with Eq. (4). Writing

$$F_1'(0) = \not{d}_1 \frac{\mu_{\rm p}}{4m_{\rm p}^2},\ \frac{1}{\kappa_{\rm p}} F_2'(0) = [\not{d}_1 - 1 - \delta_P] \frac{\mu_{\rm p}}{4m_{\rm p}^2}, \tag{11}$$

then $b_{\rm M}^{\perp} > b_{\rm E}^{\perp}\ \forall \delta_P > -1$ and Eq. (4) is recovered with $\delta_P = 0$. Working with the radii discussed above, the combinations of Eqs. (7) and (10), Eqs. (5) and (10), Eqs. (5) and (6) yield the results drawn in Fig. 3; namely:

$$\delta_P^{\text{A1SPM}} = 0.546 \pm 0.366, \tag{12a}$$
$$\delta_P^{\text{A1SPM+PDG}} = 0.329 \pm 0.321, \tag{12b}$$
$$\delta_P^{\text{PDG}} = -0.147 \pm 0.322, \tag{12c}$$

of which the uncertainty-weighted average is $\delta_P = 0.218 \pm 0.193$.

Since the low-Q^2 behavior of $[1 - \mu_{\rm p} G_{\rm E}(Q^2)/G_{\rm M}(Q^2)]$ is proportional to δ_P, greater accuracy might be achieved through new high-precision low-Q^2 polarization-transfer measurements of $\mu_{\rm p} G_{\rm E}(Q^2)/G_{\rm M}(Q^2)$, as also remarked elsewhere.[19]

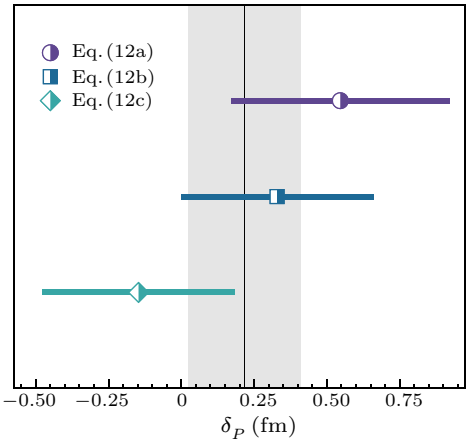

Fig. 3. Experiment-based results for deviations ($\delta_P \neq 0$) from Eq. (4) as listed in Eqs. (12). The vertical grey line together with the associated band show the uncertainty-weighted average.

5. Discussion and Conclusions. Figure 3 reveals that analyses of available data are consistent with Eq. (4) at a 26% confidence level. Namely, they suggest with this probability that the proton's Dirac and Pauli radii are not truly independent observables; instead, their difference is completely fixed by the proton Foldy term.[18] At worst, Eq. (4) is established as a useful approximation. Moreover, the analyses indicate with great certainty that the proton's Pauli radius is larger than its Dirac radius. These conclusions will serve as valuable constraints on pictures of proton structure.

Their importance is elevated by the fact that any discussion of the "size" of the "absolutely" stable proton leads naturally to a discussion of confinement.[60,61] Namely, the empirical fact that the gluon and quark quanta associated with the fields

used to define quantum chromodynamics (QCD), the strong interaction part of the Standard Model, have never been observed in a detector. Confinement has been linked with the phenomenon of emergent hadron mass (EHM),[62–64] viz., the appearance of nuclear-size masses for strong interaction systems comprised of massless field quanta.

The QCD proton is just such a bound state: seeded by three light valence quarks, i.e., two u quarks and one d quark, which are all massless in the absence of Higgs boson couplings into QCD. Symmetries in quantum field theory entail that a massless fermion cannot possess an anomalous magnetic moment;[65–67] and, in the absence of any strong corrections, the anomalous magnetic moment of a light fermion is small. Yet, the proton's Pauli form factor, which expresses all its anomalous magnetic properties, is large on $Q^2 \simeq 0$ and has a radius fixed (perhaps approximately) by Eq. (4).

An explanation for the infrared scale of F_2-proton may be found in EHM:[62–64] realized most fundamentally in QCD via the dynamical generation of running masses for gluons, i.e., QCD's gauge bosons, and quarks;[68–70] and expressed in manifold corollaries.[70–72] For example, the running masses that owe to EHM are large at infrared momenta, with that of the quark being $\sim m_{\rm p}/3$, and the same phenomenon also endows dressed light quarks with anomalous magnetic moments that are $\sim\kappa_{\rm p}/3$ in the infrared. This explains the size of $F_2(0)$. Given then Eq. (4), even as an approximation, the amount by which the proton's light-front transverse mean-square magnetic radius exceeds the analogous charge radius is also seen to be (predominantly) determined by EHM. (Numerous theory analyses indicate that EHM also strongly influences $F_1(Q^2)$, with effects flowing into both the proton wave function and electromagnetic current via the running light quark masses.[8–11])

This discussion suggests that the scales underlying the proton's anomalous magnetization form factor may be attributed to EHM. Lacking, however, is quantitatively precise theory that can match QCD with Eqs. (4) and (12). There are many possible contributions to $F_2(Q^2 \simeq 0)$, including:[7–11,73–78] quark anomalous magnetic moments, quark orbital angular momentum within the proton, meson cloud contributions to one or both, etc.; and related influences on $F_1(Q^2 \simeq 0)$. An insightful understanding of the accuracy of Eq. (4) will demand an explanation of how all these factors might combine to produce a simple algebraic outcome; and, in step with that, experiments and associated analyses that deliver a precise result for $r_{\rm M}$ so that a veracious benchmark is provided.

Acknowledgments. We are thankful for constructive comments from L. Chang, J. Friedrich, D. W. Higinbotham, R. J. Holt, V. Mokeev, W.-D. Nowak and J. Segovia. Use of the computer clusters at the Nanjing University Institute for Nonperturbative Physics is gratefully acknowledged.

References

[1] Streater R F and Wightman A S 1980 *PCT, Spin and Statistics and All That* 3rd edn (New York: W. A. Benjamin, Inc.)
[2] Pauli W 1940 *Phys. Rev.* **58** 716
[3] Weinberg S 2005 *The Quantum Theory of Fields* (Cambridge: Cambridge University Press) vol 1
[4] Coester F 1992 *Prog. Part. Nucl. Phys.* **29** 1
[5] Zyla P *et al.* 2020 *Review of Particle Physics, PTEP* **2020** 083C01
[6] Hofstadter R 1956 *Rev. Mod. Phys.* **28** 214
[7] Punjabi V, Perdrisat C F, Jones M K, Brash E J and Carlson C E 2015 *Eur. Phys. J. A* **51** 79
[8] Cloet I C and Roberts C D 2014 *Prog. Part. Nucl. Phys.* **77** 1
[9] Eichmann G, Sanchis-Alepuz H, Williams R, Alkofer R and Fischer C S 2016 *Prog. Part. Nucl. Phys.* **91** 1
[10] Brodsky S J *et al.* 2020 *Intern. J. Mod. Phys. E* **124** 2030006
[11] Barabanov M Y *et al.* 2021 *Prog. Part. Nucl. Phys.* **116** 103835
[12] Sachs R 1962 *Phys. Rev.* **126** 2256
[13] Miller G A 2010 *Ann. Rev. Nucl. Part. Sci.* **60** 1
[14] Aoyama T, Hayakawa M, Kinoshita T and Nio M 2012 *Phys. Rev. Lett.* **109** 111807
[15] Aoyama T, Hayakawa M, Kinoshita T and Nio M 2012 *Phys. Rev. Lett.* **109** 111808
[16] Frisch R and Stern O 1933 *Z. Phys.* **85** 4
[17] Jones M K *et al.* 2000 *Phys. Rev. Lett.* **84** 1398
[18] Foldy L L 1958 *Rev. Mod. Phys.* **30** 471
[19] Miller G A, Piasetzky E and Ron G 2008 *Phys. Rev. Lett.* **101** 082002
[20] Pohl R *et al.* 2010 *Nature* **466** 213
[21] Antognini A *et al.* 2013 *Science* **339** 417
[22] Beyer A *et al.* 2017 *Science* **358** 79
[23] Xiong W *et al.* 2019 *Nature* **575** 147
[24] Bezginov N, Valdez T, Horbatsch M, Marsman A, Vutha A C and Hessels E A 2019 *Science* **365** 1007
[25] Grinin A, Matveev A, Yost D C, Maisenbacher L, Wirthl V, Pohl R, Hänsch T W, Udem T 2020 *Science* **370** 1061
[26] Pohl R *et al.* 2016 *Science* **353** 669
[27] Bernauer J C *et al.* 2010 *Phys. Rev. Lett.* **105** 242001
[28] Bernauer J C *et al.* 2014 *Phys. Rev. C* **90** 015206
[29] Lee G, Arrington J R and Hill R J 2015 *Phys. Rev. D* **92** 013013
[30] Alarcón J M, Higinbotham D W and Weiss C 2020 *Phys. Rev. C* **102** 035203
[31] Lin Y H, Hammer H W and Meißner U G 2021 *Eur. Phys. J. A* **57** 255
[32] Djukanovic D, Harris T, von Hippel G, Junnarkar P M, Meyer H B, Mohler D, Ottnad K, Schulz T, Wilhelm J and Wittig H 2021 *Phys. Rev. D* **103** 094522
[33] Schlessinger L 1968 *Phys. Rev.* **167** 1411
[34] Schlessinger L and Schwartz C 1966 *Phys. Rev. Lett.* **16** 1173
[35] Tripolt R A, Haritan I, Wambach J and Moiseyev N 2017 *Phys. Lett. B* **774** 411
[36] Gao H and Vanderhaeghen M 2021 arXiv:2105.00571 [hep-ph]
[37] Kraus E, Mesick K E, White A, Gilman R and Strauch S 2014 *Phys. Rev. C* **90** 045206
[38] Lorenz I T and Meißner U G 2014 *Phys. Lett. B* **737** 57
[39] Griffioen K, Carlson C and Maddox S 2016 *Phys. Rev. C* **93** 065207
[40] Higinbotham D W, Kabir A A, Lin V, Meekins D, Norum B and Sawatzky B 2016 *Phys. Rev. C* **93** 055207
[41] Hayward T B and Griffioen K A 2020 *Nucl. Phys. A* **999** 121767
[42] Zhou S, Giulani P, Piekarewicz J, Bhattacharya A and Pati D 2019 *Phys. Rev. C* **99** 055202
[43] Alarcón J M, Higinbotham D W, Weiss C and Ye Z 2019 *Phys. Rev. C* **99** 044303
[44] Barcus S K, Higinbotham D W and McClellan R E 2020

Phys. Rev. C **102** 015205
[45] Hammer H W and Meißner U G 2020 *Sci. Bull.* **65** 257
[46] Cui Z F, Binosi D, Roberts C D and Schmidt S M 2021 *Phys. Rev. Lett.* **127** 092001
[47] Cui Z F, Binosi D, Roberts C D and Schmidt S M 2021 *Phys. Lett. B* **822** 136631
[48] Chen C, Lu Y, Binosi D, Roberts C D, Rodríguez-Quintero J and Segovia J 2019 *Phys. Rev. D* **99** 034013
[49] Binosi D, Chang L, Ding M, Gao F, Papavassiliou J and Roberts C D 2019 *Phys. Lett. B* **790** 257
[50] Binosi D and Tripolt R A 2020 *Phys. Lett. B* **801** 135171
[51] Eichmann G, Duarte P, Peña M P and Stadler A 2019 *Phys. Rev. D* **100** 094001
[52] Yao Z Q, Binosi D, Cui Z F, Roberts C D, Xu S S and Zong H S 2020 *Phys. Rev. D* **102** 014007
[53] Yao Z Q, Binosi D, Cui Z F and Roberts C D 2021 *Phys. Lett. B* **818** 136344
[54] Cui Z F, Gao F, Binosi D, Chang L, Roberts C D and Schmidt S M 2021 arXiv:2108.11493 [hep-ph]
[55] Rosenbluth M 1950 *Phys. Rev.* **79** 615
[56] Reinsch C H 1967 *Numer. Math.* **10** 177
[57] Press W H, Teukolsky S A, Vetterling W T and Flannery B P 2007 *Numerical Recipes* 3rd edn (New York: Cambridge University Press)
[58] Friedrich J and Walcher T 2003 *Eur. Phys. J. A* **17** 607
[59] Yan X, Higinbotham D W, Dutta D, Gao H, Gasparian A, Khandaker M A, Liyanage N, Pasyuk E, Peng C and Xiong W 2018 *Phys. Rev. C* **98** 025204
[60] Roberts C D, Williams A G and Krein G 1992 *Int. J. Mod. Phys. A* **7** 5607
[61] Jaffe A M 2006 *Not. Am. Math. Soc.* **53** 652
[62] Aguilar A C *et al.* 2019 *Eur. Phys. J. A* **55** 190
[63] Roberts C D 2020 *Symmetry* **12** 1468
[64] Roberts C D 2021 *AAPPS Bull.* **31** 6
[65] Singh J 1985 *Phys. Rev. D* **31** 1097
[66] Bicudo P J A, Ribeiro J E F T, Fernandes R 1999 *Phys. Rev. C* **59** 1107
[67] Chang L, Liu Y X and Roberts C D 2011 *Phys. Rev. Lett.* **106** 072001
[68] Aguilar A C, Binosi D and Papavassiliou J 2016 *Front. Phys. Chin.* **11** 111203
[69] Fischer C S 2019 *Prog. Part. Nucl. Phys.* **105** 1
[70] Roberts C D, Richards D G, Horn T and Chang L 2021 *Prog. Part. Nucl. Phys.* **120** 103883
[71] Qin S X and Roberts C D 2021 *Chin. Phys. Lett.* **38** 071201
[72] Arrington J *et al.* 2021 *J. Phys. G* **48** 075106
[73] Giannini M M and Santopinto E 2015 *Chin. J. Phys.* **53** 020301
[74] Sufian R S, de Téramond G F, Brodsky S J, Deur A and Dosch H G 2017 *Phys. Rev. D* **95** 014011
[75] Xu Y Z, Binosi D, Cui Z F, Li B L, Roberts C D, Xu S S and Zong H S 2019 *Phys. Rev. D* **100** 114038
[76] Mondal C, Xu S, Lan J, Zhao X, Li Y, Chakrabarti D and Vary J P 2020 *Phys. Rev. D* **102** 016008
[77] Cui Z F, Chen C, Binosi D, de Soto F, Roberts C D, Rodríguez-Quintero J, Schmidt S M and Segovia J 2020 *Phys. Rev. D* **102** 014043
[78] Xu Y Z, Chen S, Yao Z Q, Binosi D, Cui Z F and Roberts C D 2021 *Eur. Phys. J. C* **81** 895